Driving Force Dependence of Electron Transfer Dynamics in Synthetic DNA Hairpins

Frederick D. Lewis,* Rajdeep S. Kalgutkar, Yansheng Wu, Xiaoyang Liu, Jianqin Liu, Ryan T. Hayes, Scott E. Miller, and Michael R. Wasielewski*

Contribution from the Department of Chemistry, Northwestern University, Evanston, Illinois 60208

Received July 31, 2000. Revised Manuscript Received October 18, 2000

Abstract: The driving force dependence of photoinduced electron-transfer dynamics in duplex DNA has been investigated for 16 synthetic DNA hairpins in which an acceptor chromophore serves as a linker connecting two complementary oligonucleotide arms containing a single donor nucleobase located either adjacent to the linker or separated from the linker by two unreactive base pairs. The rate constants for both charge separation and charge recombination processes have been determined by means of subpicosecond time-resolved transient absorption spectroscopy and the results analyzed using quantum mechanical Marcus theory. This analysis provides intimate details about electron-transfer processes in DNA including the distance dependence of the electronic coupling between the acceptor and nucleobase donor and the solvent and nuclear reorganization energies.

Introduction

Charge-transfer processes play a crucial role in chemical, radiolytic, and photochemical reactions leading to the oxidative damage of DNA.[1,2] During the past several years significant progress has been made toward elucidation of the mechanism and dynamics of photoinduced charge-transfer processes in DNA.[3] Experiment and theory have converged in the elucidation of two mechanisms for charge transfer in DNA, a single step superexchange mechanism that is strongly distance dependent[4−9] and a multistep hopping mechanism that is only weakly distance dependent.[9−14] Investigations of the dynamics of these processes to date have focused on their distance dependence. Several studies of the distance dependence of single-step charge-transfer processes in DNA have shown that they can be described in simplest form by eq 1, where *R* is the D−A center-to-center distance and β is dependent upon the nature of the bridge and its coupling with D and A.[15]
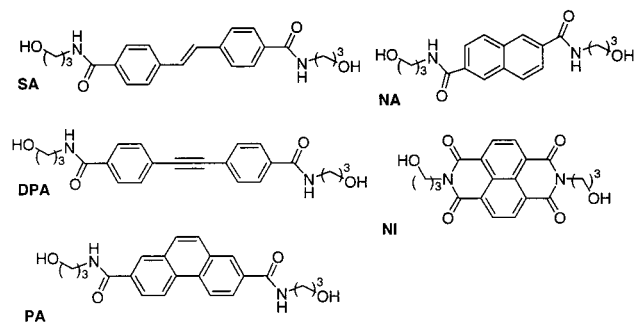
$$k_{cs} = k_o e^{-\beta R} \tag{1}$$

The dynamics of charge-transfer processes in DNA are also expected to be dependent upon the thermodynamic driving force, in accord with Marcus electron transfer theory.[16] There have been numerous studies of the driving force dependence of charge-transfer dynamics both in donor−acceptor (D−A) systems which form contact or solvent-separated ion pairs[17−23] and in donor−bridge−acceptor (D−B-A) systems.[24−27] The bridges investigated include proteins, saturated hydrocarbons, and conjugated unsaturated oligomers and display values of β ranging from 1.4 to <0.1. To our knowledge the driving force dependence of charge transfer in cofacial π-donor acceptor systems has been investigated in only one system, the cyclophane-bridged porphyrin−quinone system investigated by Staab and Michel-Beyerle,[21,22] and there have been no studies of π-stacked D−B−A systems.

We report here the results of our investigation of the driving force dependence of the dynamics of photoinduced electron-transfer processes in hairpin-forming bis(oligonucleotide) conjugates in which an organic chromophore serves as a linker connecting two complementary oligonucleotides. The acceptor

* Address correspondence to either author. E-mail: lewis@chem.nwu.edu or wasielew@chem.nwu.edu.

(1) Armitage, B. *Chem. Rev.* **1998**, *98*, 1171−1200.
(2) Burrows, C. J.; Muller, J. G. *Chem. Rev.* **1998**, *98*, 1109−1151.
(3) Grinstaff, M. W. *Angew. Chem., Int. Ed.* **1999**, *38*, 3629−3635.
(4) Lewis, F. D.; Wu, T.; Zhang, Y.; Letsinger, R. L.; Greenfield, S. R.; Wasielewski, M. R. *Science* **1997**, *277*, 673−676.
(5) Lewis, F. D.; Wu, T.; Liu, X.; Letsinger, R. L.; Greenfield, S. R.; Miller, S. E.; Wasielewski, M. R. *J. Am. Chem. Soc.* **2000**, *122*, 2889−2902.
(6) Fukui, K.; Tanaka, T. *Angew. Chem., Int. Ed.* **1998**, *37*, 158−161.
(7) Harriman, A. *Angew. Chem., Int. Ed.* **1999**, *38*, 945−949.
(8) Priyadarshy, S.; Risser, S. M.; Beratan, D. N. *J. Phys. Chem.* **1996**, *100*, 17678−17682.
(9) Jortner, J.; Bixon, M.; Langenbacher, T.; Michel-Beyerle, M. E. *Proc. Natl. Acad. Sci. U.S.A.* **1998**, *95*, 12759−12765.
(10) Giese, B. *Acc. Chem. Res.* **2000**, *33*, 631−636.
(11) Schuster, G. B. *Acc. Chem. Res.* **2000**, *33*, 253−260.
(12) Lewis, F. D.; Liu, X.; Liu, J.; Miller, S. E.; Hayes, R. T.; Wasielewski, M. R. *Nature* **2000**, *406*, 51−53.
(13) Bixon, M.; Giese, B.; Wessely, S.; Langenbacher, T.; Michel-Beyerle, M. E.; Jortner, J. *Proc. Natl. Acad. Sci. U.S.A.* **1999**, *96*, 11713−11716.
(14) Berlin, Y. A.; Burin, A. L.; Ratner, M. A. *J. Phys. Chem. A* **2000**, *104*, 443−445.
(15) Bixon, M.; Jortner, M. *Adv. Chem. Phys.* **1999**, *106*, 35−202.

(16) Marcus, R. A. *J. Chem. Phys.* **1956**, *24*, 966−978.
(17) Asahi, T.; Mataga, N. *J. Phys. Chem.* **1991**, *95*, 1956−1963.
(18) Asahi, T.; Ohkohchi, M.; Mataga, N. *J. Phys. Chem.* **1993**, *97*, 13132.
(19) Gould, I. R.; Farid, S. *Acc. Chem. Res.* **1996**, *29*, 522−528.
(20) Hubig, S. M.; Bockman, T. M.; Kochi, J. K. *J. Am. Chem. Soc.* **1996**, *118*, 3842−3851.
(21) Häberle, T.; Hirsch, J.; Pöllinger, F.; Heitele, H.; Michel-Beyerle, M. E.; Anders, C.; Döhling, A.; Krieger, C.; Rückermann, A.; Staab, H. A. *J. Phys. Chem.* **1996**, *100*, 18269−18274.
(22) Pöllinger, F.; Musewald, C.; Heitele, H.; Michele-Beyerle, M. E. *Ber. Bunsen-Ges. Phys. Chem.* **1996**, *100*, 2076−2080.
(23) Bixon, M.; Jortner, J.; Cortes, J.; Heitele, H.; Michel-Beyerle, M. E. *J. Phys. Chem.* **1994**, *98*, 7289−7299.
(24) Closs, G. L.; Miller, J. R. *Science* **1988**, *240*, 440−447.
(25) Winkler, J. R.; Gray, H. B. *Chem. Rev.* **1992**, *92*, 369−379.
(26) Wasielewski, M. R. *Chem. Rev.* **1992**, *92*, 435−461.
(27) Wasielewski, M. R.; Niemczyk, M. P.; Svec, W. A.; Pewitt, E. B. *J. Am. Chem. Soc.* **1985**, *107*, 1080−1082.

Electron Transfer Dynamics in Synthetic DNA Hairpins

J. Am. Chem. Soc., Vol. 122, No. 49, 2000 12347

Chart 1. Structures of Linker Diols

Table 1. Singlet Energies, Singlet Decay Times, and Reduction Potentials of Linker Diols

linker[a]	E_S, eV[b]	τ_S, ns[c]	E_{rdn}, V[d]
SA	3.35	2.0	−1.91
NA	3.55	12.0	−2.05
DPA	3.76	0.22	−1.98
PA	3.35	18.4	−2.16
NI	3.24	e	−0.55

[a] See Chart 1 for structures. [b] Singlet energy estimated from the crossing point of the fluorescence emission and excitation spectra in methanol solution. [c] Singlet decay time in deoxygenated methanol solution. [d] Reduction potential in DMSO solution vs SCE. [e] Nonfluorescent in methanol.

Chart 2. Structures and Oxidation Potentials (vs SCE) of the Nucleobases

linker and donor nucleobase are located either adjacent to each other or separated by two T:A base pairs, thus permitting the investigation of charge-transfer processes in both a D−A and D−B−A system with a π-stacked base-pair bridge. The dynamics of charge separation and charge recombination processes have been determined by means of time-resolved transient absorption spectroscopy with subpicosecond time resolution[5] and the results of these measurements analyzed by means of quantum mechanical Marcus theory for electron transfer.[15,28,29] This analysis provides heretofore unavailable information about electron-transfer processes in DNA.
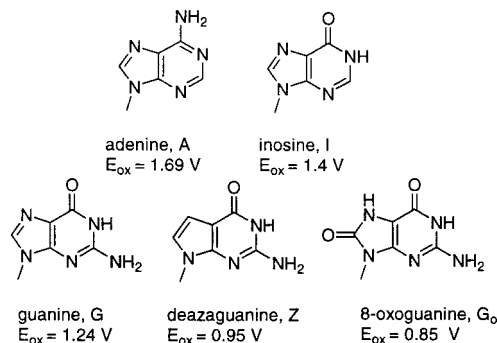
Results

The organic chromophore linkers used in the synthesis of hairpin-forming bis(oligonucleotide) conjugates were prepared from the di(hydroxypropyl)-chromophore derivatives shown in Chart 1 using the method of Letsinger and co-workers.[30,31] The syntheses of the linker diols of stilbene-4,4′-dicarboxamide (SA),[31] naphthalene-2,6-dicarboxamide (NA),[32] and diphenylacetylene-4,4′-dicarboxamide (DPA)[33] have been previously described. The linker diol derived from phenanthrene-2,7-dicarboxamide (PA) was prepared via oxidative photocyclization of stilbene-3,3′-dicarboxamide and the diol derived from 1,4:5,8-naphthalene diimide (NI) was prepared via the reaction of the dianhydride with 3-aminopropanol (see the Experimental Section). The linker diols are all strongly fluorescent in both nonpolar and polar solvents, except for NI which is fluorescent in nonpolar solvents but not in methanol. The linker singlet energies, singlet lifetimes, and reduction potentials are reported in Table 1.[34]

Bis(oligonucleotide) conjugates are prepared via conventional phosphoramidite chemistry using the monoprotected (as the (4,4′-dimethoxytriphenylmethyl)ether derivative), monoactivated (as the phosphoramidite) diol derivatives.[31] In the case of the NI linker the modified procedure of Bevers et al.[35] was used. In addition to the four common nucleobases, the nucleobase analogues ionosine, deazaguanine, and 8-oxoguanine have been employed. The structures, letter codes, and oxidation potentials of the nucleobases are provided in Chart 2.[36,37] The structures of hairpins in which the donor nucleobase is adjacent to the

linker or separated from the linker by two T:A base pairs are shown schematically in Chart 3. Hairpins **1**−**16** investigated in this study are listed by number in Table 2 and are identified by the linker and the donor base pair and its location.

Molecular modeling[5] indicates that these hairpins can adopt B-form structures in which the linker chromophore is approximately parallel to the adjacent base pair, similar to the structure of a stilbene diether-linked hairpin which has been determined crystallographically.[38] Minimized structures for hairpins **5** and **13** which possess a stilbene linker and guanine donor are shown in Chart 3. The calculated chromophore−base pair plane-to-plane separations have values of 3.8 ± 0.3 Å, which are dependent upon the choice of linker. This is slightly larger than the 3.4 Å average distance between base pairs in B-form DNA. The hairpins all have melting temperatures greater than 55 °C in 0.1 M NaCl, pH 7.2, buffer solution. Their absorption, circular dichroism, and fluorescence spectra show no evidence for significant ground-state interaction between the linker chromophore and adjacent base pair. The fluorescence decay times of hairpins **1** and **3** are 25 and 2.0 ns, respectively, longer than those of the PA and SA diols (Table 1). The linker fluorescence is quenched to a greater or lesser extent in all of the other hairpins investigated.

Transient absorption spectra for several hairpins containing the SA or DPA linker have been previously reported.[4,5,33] At short delay times (1−2 ps) following the pump pulse the spectra of hairpins **4**, **7**, and **12**−**15** (Table 1) resemble those of the unconjugated SA or DPA linker and are assigned to the linker singlet state. The band shape and band maxima change with time to those of the anion radicals SA$^{-\bullet}$ and DPA$^{-\bullet}$. In the case

(28) Ulstrup, J.; Jortner, J. *J. Chem. Phys.* **1975**, *63*.

(29) Jortner, J. *J. Chem. Phys.* **1976**, *64*, 4860−4867.

(30) Salunkhe, M.; Wu, T.; Letsinger, R. L. *J. Am. Chem. Soc.* **1992**, *114*, 8768−8772.

(31) Letsinger, R. L.; Wu, T. *J. Am. Chem. Soc.* **1995**, *117*, 7323−7328.

(32) Lewis, F. D.; Zhang, Y.; Liu, X.; Xu, N.; Letsinger, R. L. *J. Phys. Chem. B* **1999**, *103*, 2570−2578.

(33) Lewis, F. D.; Liu, X.; Miller, S. E.; Wasielewski, M. R. *J. Am. Chem. Soc.* **1999**, *121*, 9746−9747.

(34) Linker singlet energies are determined from the intersection of absorption and fluorescence spectra. Linker oxidation potentials are measured vs SCE in dimethyl sulfoxide solution.

(35) Bevers, S.; O'Dea, T. P.; McLaughlin, L. W. *J. Am. Chem. Soc.* **1998**, *120*, 11004−11005.

(36) Oxidation potentials are for the nucleosides in acetonitrile solution vs SCE. Values for T, C, A, and G are from ref 37. Values for the other nucleobases are from several literature sources and are reported relative to the value for G.

(37) Seidel, C. A. M.; Schulz, A.; Sauer, M. H. M. *J. Phys. Chem.* **1996**, *100*, 5541−5553.

(38) Lewis, F. D.; Liu, X.; Wu, Y.; Miller, S. E.; Wasielewski, M. R.; Letsinger, R. L.; Sanishvili, R.; Joachimiak, A.; Tereshko, V.; Egli, M. *J. Am. Chem. Soc.* **1999**, *121*, 9905−9906.

Chart 3. Structures of Hairpins with (a) Nearest-Neighbor and (b) Bridge-Mediated Nucleobase Quenchers[a]

(a)

L = NA, PA, SA, DPA, or NI
X--Y = A:T, I:C, G:C, or Z:C

(b)

L = PA or SA
X--Y = I:C, G:C, Z:C, or G_0-C
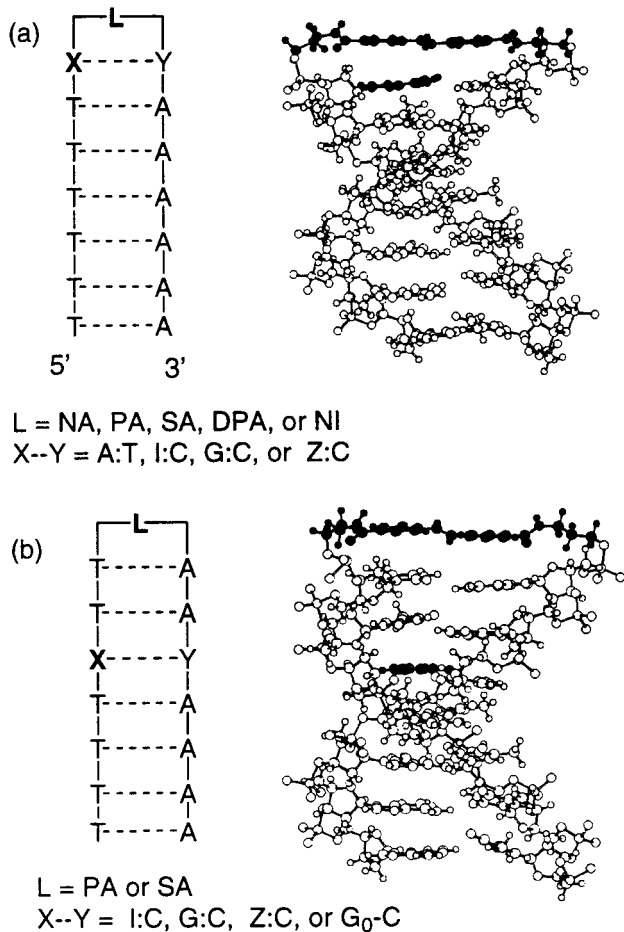
[a] Minimized structures are those of hairpins **3** (a) and **13** (b) which possess SA linkers and guanine quenchers shown with darker spheres.

Table 2. Energetics and Kinetics of Charge Separation and Charge Recombination

hairpin[a]	$-\Delta G_{cs}$, eV[b]	k_{cs}, s^{-1} [c]	$-\Delta G_{cr}$, eV[d]	k_{cr}, s^{-1} [e]
1: PA-1A:T	−0.50	$<1 \times 10^{7f}$		
2: NA-1A:T	−0.19	3.0×10^{9f}		
3: SA-1A:T	−0.25	$<1 \times 10^{8f}$		
4: SA-1I:C	0.04	5.5×10^{10}	3.28	3.5×10^{9}
5: SA-1G:C	0.20	1.0×10^{12}	3.13	4.3×10^{10}
6: SA-1Z:C	0.49	5.0×10^{12}	2.83	7.1×10^{10}
7: DPA-1A:T	0.09	3.7×10^{11}	3.67	7.1×10^{8}
8: DPA-1I:C	0.38	7.7×10^{11}	3.45	9.8×10^{9}
9: DPA-1G:C	0.54	2.5×10^{12}	3.20	5.2×10^{10}
10: NI-1A:T	1.00	7.3×10^{12}	2.24	2.5×10^{11}
11: NI-1G:C	1.45	4.5×10^{12}	1.79	5.0×10^{11}
12: SA-3I:C	0.04	1.7×10^{8}	3.28	1.1×10^{8}
13: SA-3G:C	0.20	8.3×10^{9}	3.13	2.6×10^{8}
14: SA-3Z:C	0.49	2.1×10^{10}	2.83	4.8×10^{8}
15: SA-3G$_0$:C	0.59	3.7×10^{10}	2.73	1.1×10^{9}
16: PA-3G:C	−0.05	2.7×10^{7f}		

[a] See Charts 1−3 for hairpin, linker, and nucleobase structures. [b] Free energy of charge separation calculated using eq 2. [c] Rate constant for charge separation obtained from the singlet state decay time obtained from transient absorption spectroscopy except as noted. [d] Free energy of charge recombination calculated using eq 3. [e] Rate constant for charge recombination obtained from the anion radical decay time. [f] Rate constant estimated from fluorescence decay data.

of hairpins **5**, **6**, **8**, and **9** formation of the anion radical is essentially complete within a few picoseconds and only the transient absorption spectrum of the anion radical is observed at delay times of 1−2 ps. Similar results are obtained for the
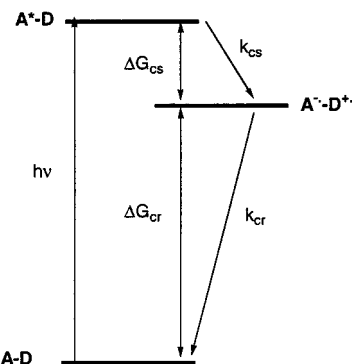
Figure 1. Kinetic scheme and thermodynamics of charge separation and charge recombination. A is the acceptor linker chromophore and D is the nucleobase donor.

hairpins **10** and **11** which possess the NI linker. The transient decays of hairpins **4**−**15** determined at a single wavelength are dual exponentials, the faster decay being assigned to singlet state charge separation ($\tau_s^{-1} = k_{cs}$) and the slower decay to anion radical charge recombination ($\tau_a^{-1} = k_{cr}$). Values of k_{cs} and k_{cr} are summarized in Table 2. In the case of hairpins **2** and **16** values of k_{cs} are determined from fluorescence decay data ($k_{cs} = \tau^{-1} - \tau_o^{-1}$) and for **1** and **3** charge separation is not observed and thus the singlet decay times provide upper limits for k_{cs} ($k_{cs} \ll \tau_o^{-1}$). The formation of the linker anion radical via a two-step process, electronic excitation followed by charge transfer, is consistent with the absence of significant perturbation of the electronic spectra of the linkers by the neighboring base pair.

Discussion

The driving force for photoinduced charge separation and charge recombination can be calculated by means of Weller's equations (eqs 2 and 3)

$$\Delta G_{cs} = E_{ox} - E_{red} - E_S + C \quad (2)$$

$$\Delta G_{cr} = E_{red} - E_{ox} \quad (3)$$

where E_{ox} is the nucleobase oxidation potential, E_{red} is the linker reduction potential, E_S is the linker singlet energy, and C is the solvent-dependent Coulombic attraction energy.[39] These thermodynamic relationships are shown schematically in Figure 1. The calculated values of ΔG_{cs} and ΔG_{cr} obtained using data from Table 1 and Chart 2 are reported in Table 2. The oxidation potentials of the nucleobases in duplex DNA have not been measured. The values reported in Chart 2 are those measured for the nucleosides in polar aprotic solvents rather than the significantly lower values measured in aqueous solution.[37,40] The use of nonaqueous potentials is consistent with the moderately polar nature of the base-paired core of DNA.[32]

The rate constants for charge separation and charge recombination (k_{cs} and k_{cr}) reported in Table 2 are obtained from either transient absorption or fluorescence decay measurements. The transient absorption and fluorescence decay data are best fit by single exponential functions for both charge separation and charge recombination processes. This indicates either that the hairpins adopt a single conformation (or an ensemble of kinetically equivalent conformations) or that conformational changes are more rapid than the charge-transfer processes. The

(39) Weller, A. *Z. Phys. Chem. Neue. Folg.* **1982**, *133*, 93−98.
(40) Steenken, S.; Jovanovic, S. V. *J. Am. Chem. Soc.* **1997**, *119*, 617−618.
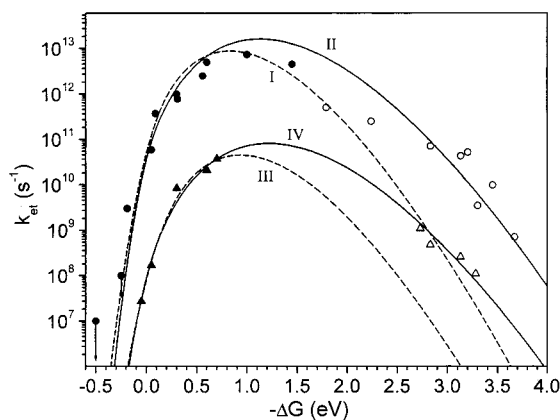
Figure 2. Free energy dependence of rate constants for charge separation (k_{cs}, filled symbols) and charge recombination (k_{cr}, empty symbols) for nearest-neighbor charge transfer ($\bullet$, $\circ$) and bridge-mediated charge transfer ($\blacktriangle$, $\triangle$). Dashed lines are fits to k_{cs} data (Fits I and III). Solid lines are global fits to k_{cs} and k_{cr} (Fits II and IV). Electron-transfer parameters obtained from these fits are reported in Table 3.

free energy dependence of the rate constants k_{cs} and k_{cr} for nearest-neighbor charge transfer in hairpins **1−11** and for bridge-mediated charge transfer in hairpins **12−16** is shown in Figure 2. Values of k_{cs} for nearest-neighbor charge separation increase rapidly from 10^7 s^{-1} for hairpin **1** ($\Delta G_{cs} = +0.5$ eV) to 5×10^{12} s^{-1} for hairpin **6** ($\Delta G_{cs} = -0.6$ eV) but remain fairly constant or decrease slightly for larger driving forces. Values of k_{cr} decrease with increasing driving force, as expected for electron-transfer processes in the Marcus inverted region.[16] Values of k_{cs} and k_{cr} are smaller for bridge-mediated vs nearest-neighbor charge transfer.

The data in Figure 2 can be analyzed within the framework of semiclassical electron transfer theory using the Marcus−Levich−Jortner equation (eq 4),

$$k_{et} = \frac{2\pi}{\hbar} \frac{H_{DA}^2}{\sqrt{4\pi\lambda_s k_B T}} e^{-S_c} \sum_{n=0}^{\infty} \frac{S_c^n}{n!} e^{-(\Delta G + \lambda_s + n\hbar\langle\omega_c\rangle)^2/(4\lambda_s k_B T)} \quad (4)$$

$$S_c = \frac{\lambda_i}{\hbar\langle\omega_c\rangle}$$

where $\hbar = h/2\pi$ (h is Planck's constant), k_B is the Boltzmann constant, T is the temperature (298 K), H_{DA} is the electronic coupling matrix element, S_c is the Huang−Rhys factor, ΔG is the free energy change (eq 2 or 3), λ_i is the nuclear reorganization energy, λ_s is the solvent reorganization energy, and $\langle\omega_c\rangle$ is the average high-frequency vibrational frequency.[15,28,29] A value of $\hbar\langle\omega\rangle = 1500$ cm^{-1} is assumed for electron-transfer processes involving aromatic molecules.[19,24]

A 3-parameter fit to the nearest-neighbor charge separation data to eq 4 (Fit I) is shown in Figure 2 and values of λ_s, λ_i, and H_{DA} reported in Table 3. The reasonable fit of the data for all of the acceptor linkers to a single curve indicates that differences in the D−A geometry or solvation do not have a large effect on the observed rates. The occurrence of the maximum in k_{cs} for a value of $\Delta G \sim 0.6$ eV is similar to that obtained for numerous D−A and D−B−A systems,[25,26] suggesting that the errors in calculating ΔG_{cs} (eq 2) using the nucleoside oxidation potentials reported in Chart 2 are small. The appearance of Fit I is similar to that reported by Staab and Michel-Beyerle[21] for the dynamics of charge separation in

Table 3. Electron Transfer Parameters from Fitting the Driving Force Dependence of the Charge Transfer Dynamics in Figure 2[a]

Fit[b]	λ_s, eV	λ_i, eV	H_{DA}, cm^{-1}
I	0.31 ± 0.18	0.61 ± 0.27	230 ± 57
II	0.23 ± 0.13	0.99 ± 0.12	347 ± 70
III	0.41 ± 0.04	0.60 ± 0.32	17 ± 3
IV	0.27 ± 0.09	1.03 ± 0.09	25 ± 4

[a] Parameters optimized with errors determined from fitting procedures using a value of $\hbar\langle\omega\rangle = 1500$ cm^{-1}. [b] (I) Fit to nearest-neighbor k_{cs} data. (II) Fit to nearest-neighbor k_{cs} and k_{cr} data. (III) Fit to bridge-mediated k_{cs} data. (IV) Fit to bridge-mediated k_{cs} and k_{cr} data. For details see text.

cyclophane-bridged porphyrin−quinone systems. Their reported values of $\lambda_s = 0.30$ eV and $\lambda_i = 0.54$ eV in nonpolar solvents are similar to those reported for Fit I (Table 3), whereas their value of $H_{DA} = 144$ cm^{-1} is somewhat smaller than our value. The relatively small values of H_{DA} indicate the absence of strong coupling in these systems, in accord with the assumption of nonadiabicity.

A unique, satisfactory fit to eq 4 cannot be obtained using the nearest-neighbor charge recombination data in Table 2. The appearance of the charge recombination data in Figure 2 is similar to that reported by Mataga and Kochi and their co-workers for charge recombination for the contact radical ion pairs formed upon the excitation of ground-state Mulliken-type charge-transfer complexes.[17,18,20] They found that the charge recombination dynamics for contact radical ion pairs can be fit by a simple energy gap law.[23] Linear plots of log(k_{cr}) vs ΔG_{cr} for several families of π-donor−acceptor complexes have slopes in the range $2.0-3.6$ eV^{-1}.[20] Our nearest-neighbor charge recombination data plotted in this fashion have a slope of 3.0 ± 0.6 eV^{-1}, well within this range. Gould and Farid[19,41] have imposed a parabolic fit on their contact radical ion pair charge recombination data and obtained an estimated value of $H_{DA} = 750-1000$ cm^{-1} from a two-parameter fit by assuming values of $\hbar\langle\omega\rangle = 1500$ cm^{-1} and $\lambda_i = 0.25$ eV.

The data for nearest-neighbor charge separation and charge recombination can also be analyzed as a single data set. The use of both k_{cs} and k_{cr} data to obtain a single set of electron-transfer parameters has been questioned based on differences in the initial and final electronic states involved.[27] However, this approach has been used successfully for porphyrin−quinone systems with rigid structures.[27,42] Staab and Michel-Beyerle[21,22,43] report similar electron-transfer parameters for fits of k_{cs} data alone or both k_{cs} and k_{cr} data for their porphyrin−quinone systems.

A global 3-parameter fit to both charge separation and charge recombination data is shown in Figure 2 (Fit II) and the resulting electron-transfer parameters reported in Table 3. The values of ΔG_{cr} calculated from the sum of the redox potentials (eq 3) may overestimate the energies of the relaxed radical ion pair states. However, scaling the ΔG_{cr} values by as much as 0.25 V has little effect upon the electron-transfer parameters obtained from the global fit. The values of k_{cr} for the strongest acceptor, NI, fall below the calculated Fit II, even though they are the fastest we have observed for charge recombination processes. It is possible that the ultimate rates of charge transfer are limited by vibrational relaxation of the radical ion pair state or by

(41) Gould, I. R.; Young, R. H.; Moody, R. E.; Farid, S. *J. Phys. Chem.* **1991**, *95*, 2068−2080.

(42) Irvine, M. P.; Harrison, R. J.; Beddard, G. S.; Leighton, P.; Sanders, J. K. M. *Chem. Phys.* **1986**, *104*, 315−324.

(43) Heitele, H.; Pöllinger, F.; Kremer, K.; Michel-Beyerle, M. E.; Futscher, M.; Voit, G.; Weiser, J.; Staab, H. A. *Chem. Phys. Lett.* **1992**, *188*, 270−278.

12350   *J. Am. Chem. Soc., Vol. 122, No. 49, 2000*

Lewis et al.

solvent dynamics. Alternatively, subtle differences in the structure or solvation of NI, which is the only diimide linker studied, and the diamide acceptor linkers might affect the charge transfer dynamics. In any event, omission of the NI data results in only small changes in the calculated electron-transfer parameters reported for Fit II in Table 3.

The k_{cs} and k_{cr} data for bridge-mediated electron transfer in hairpins **12**−**16** are also shown in Figure 2. The electron-transfer parameters obtained from 3-parameter fits of the k_{cs} data (Fit III) and of the global fit to the combined k_{cs} and k_{cr} data (Fit IV) are reported in Table 3. As is the case for nearest-neighbor charge transfer, the fit to k_{cs} (Fit III) provides the larger value of λ_s and the global fit the larger values for λ_i and H_{DA}. The value of H_{DA} is expected to decrease exponentially with increasing donor−acceptor separation according to eq 5, where

$$H_{DA} = H_{DA}{}^{o} \exp(-\beta(R - R_{o})/2) \qquad (5)$$

β is the distance dependence of the bridge-mediated electron-transfer process, R is the interplanar distance, and $R_o = 3.4$ Å, the DNA π-stacking distance.[15] Using the values of H_{DA} for nearest-neighbor charge transfer ($R - R_o = 0.4$ Å) and bridge-mediated charge transfer ($R - R_o = 7.2$ Å) from the global Fits II and IV values of $\beta = 0.77$ Å^{-1} and $H_{DA}{}^{o} = 400$ cm^{-1} are obtained. To our knowledge, this is the first use of H_{DA} values determined from rate vs ΔG data for two fixed donor−acceptor distances to determine β and $H_{DA}{}^{o}$. The value of β is intermediate between the values previously obtained from the distance dependence of the dynamics of charge separation ($\beta = 0.7$ Å^{-1}) and charge recombination ($\beta = 0.9$ Å^{-1}),[5] in accord with the use of both k_{cs} and k_{cr} data to determine H_{DA}.

The pronounced distance dependence of H_{DA} can account in part for the larger value obtained from our nearest-neighbor data and that reported for the cyclophane-bridged porphyrin−quinone systems (347 and 133 cm^{-1}, respectively, for the global fits) since the estimated donor−acceptor separation is smaller for the DNA hairpins (3.8 Å vs 4.5 Å).[21] Our value of $H_{DA}{}^{o} = 400$ cm^{-1} is distinctly smaller than the value of 750−1000 cm^{-1} estimated by Gould and Farid[19,41] from an imposed 2-parameter fit of their radical ion pair charge recombination data. Harriman[7] has recently reported values of H_{DA} for DNA electron transfer between an intercalated donor and acceptor calculated from the temperature dependence of k_{cs} using classical Marcus theory. The value of $H_{DA} = 4.4$ cm^{-1} for three intervening base pairs ($R - R_o = 10.2$ Å) is similar to that obtained by extrapolation of our results to this distance ($H_{DA} = 8.0$ cm^{-1}).

There are several notable features of the electron-transfer parameters reported in Table 3 in addition to the magnitude and distance dependence of H_{DA}. The values of λ_s, the solvent reorganization energy, for bridge-mediated charge transfer (Fits III and IV) are only slightly larger than those for nearest-neighbor charge transfer (Fits I or II). The values of λ_s for nearest-neighbor charge transfer are similar to the value reported for cofacial porphyrin−quinone systems in nonpolar and polar solvents ($\lambda_s = 0.26$ eV in either hexane or acetonitrile).[21] A larger value of λ_s was reported by Gould and Farid[19] for the charge recombination of contact radical ion pairs ($\lambda_s = 0.48$ eV in acetonitrile). The smaller values of λ_s for the hairpin and porphyrin−quinone systems plausibly reflect their compact structures which limit contact of the donor and acceptor with the solvent.

The values of λ_i, the nuclear reorganization energy, are similar for nearest-neighbor and bridge-mediated electron transfer, based on a comparison of either the fits to k_{cs} (Fits I and III) or the

global fits to k_{cs} and k_{cr} (Fits II and IV). This suggests that changes in the geometry of the linker chromophore and adjacent base pair are more important than changes in base pair stacking and is consistent with slow motion of the base pairs on the time scale of the charge-transfer processes. The values of λ_i obtained from Fits I and III are similar to those reported by Staab and Michel-Beyerle for the porphyrin−quinone system ($\lambda_i = 0.53$ eV).[21] Verhoeven and Paddon-Row[44,45] have proposed a similar value ($\lambda_i = 0.60$ eV) for D−B−A systems with rigid σ-bonded bridges. The larger values of λ_i obtained from the global fits to our data (Fits II and IV) may reflect the conformational mobility of the hairpin loop region.

In summary, analysis of the driving force dependence of the dynamics of charge transfer in DNA hairpins using Marcus−Jortner−Levich theory[15,28,29] provides new insights into the behavior of the π-stacked nucleobases in DNA. Nearest-neighbor charge transfer is characterized by a moderately large electronic coupling matrix element and nuclear reorganization energy and a relatively small solvent reorganization energy. These properties can be attributed to the compact π-stacked geometry of the DNA hairpin loop region. Bridge-mediated charge transfer is characterized by a substantially smaller electronic coupling matrix element but only small changes in the solvent and nuclear reorganization energies. Thus the exponential distance dependence of the charge-transfer rate constants on D−A distances originates from changes in the electronic coupling rather than the solvent or nuclear reorganization energies. Finally, the distance dependence of the electronic coupling matrix element confirms that the π-stacked bases in DNA provide a somewhat better medium for electron transfer than do σ-bonded bridges, but that DNA does not function as a molecular wire.

Experimental Section

General. Methods for the preparation, purification, and characterization of (bis)oligonucleotide conjugates and the investigation of their steady state and transient absorption spectroscopy have been previously described.[5] Transient spectra were obtained using 340 nm excitation for SA and NI linkers and 327 nm excitation for DPA linkers. Decays were monitored at 575 nm for SA, 500 nm for DPA, and 460 nm for NI linkers.

***N,N′*-[Bis(3-hydroxypropyl)]-2,7-phenanthrenedicarboxamide, PA.** Stilbene-3,3′-dicarboxylic acid was prepared as a mixture of cis- and trans-isomers via the reaction of 3-formylbenzoic acid with the Wittig salt obtained from reaction of 3-(chloromethyl)benzoic acid with triphenylphosphine. A solution of the dicarboxylic acid (2.24 g) in 500 mL of tetrahydrofuran containing 100 mg of iodine was irradiated for 10 h with a 450-W mercury arc in a quartz well while air was slowly bubbled through the solution. The resulting precipitate was collected and dried, giving phenanthrene-2,7-dicarboxylic acid (0.8 g). ^{1}H NMR (DMSO-d_6) 9.0 (d, 2H), 8.68 (d, 2h), 8.22 (dd, 2H), 8.10 (s, 2H). A suspension of phenanthrene-2,7-dicarboxylic acid (424.7 mg) in benzene (20 mL), dichloroethane (40 mL), and thionyl chloride (0.6 mL) was refluxed overnight. Removal of the solvent at reduced pressure provided the diacid chloride as a yellow solid. Tetrahydrofuran (20 mL) was added and the resulting suspension was slowly poured into a well-stirred solution of 3-aminopropanol (0.4 mL) and triethylamine (2 mL) in methanol (20 mL) at 0 °C, and this mixture warmed to room temperature and stirred overnight. The solvent was removed and the resulting white solid washed with water and methanol (528 mg, 87% yield). ^{1}H NMR (DMSO-d_6, ppm) 8.72 (t, 2H), 8.95 (d, 2H),

(44) Overing, H.; Paddon-Row, M. N.; Heppener, M.; Oliver, A. M.; Cotsaris, E.; Verhoeven, J. W.; Hush, N. S. *J. Am. Chem. Soc.* **1987**, *109*, 3258−3269.

(45) Kroon, J.; Verhoeven, J. W.; Paddon-Row, M. N.; Oliver, A. M. *Angew. Chem., Int. Ed.* **1991**, *30*, 1358−1361.

8.52 (d, 2H), 8.14 (dd, 2H), 7.98 (s, 2H), 4.53 (t, 2H), 3.50 (t, 4H), 3.40 (m, 4H), 1.74 (m, 4H).

N,N′-[Bis(3-hydroxypropyl)]-1,4:5,8-naphthalimide, NI. To a suspension of 1,4,5,8-naphthalenetetracarboxylic acid dianhydride (2.0 g) in 20 mL of anhydrous *N,N*-dimethylacetamide (DMA) was added dropwise with stirring a solution of 1.4 mL of 3-aminopropanol in DMA. The reaction mixture was heated at 120 °C for 2 h and then vacuum distilled to remove the solvent. The residue was collected and recrystallized from pyridine affording pink needles (1.7 g, 62%). This material was further purified by column chromatography (silica gel, dichloromethane:methanol elutant) providing yellow crystals (Rf: 0.36 10% MeOH/CH$_2$Cl$_2$). ^{1}H NMR (DMSO-d_6, ppm) 8.65 (s, 4H), 4.54 (t, 2H), 4.12 (m, 4H), 3.53 (t, 4H), 1.82 (m, 4H).

JA0028267